High-Density Single Nucleotide Polymorphism Array Defines Novel Stage and Location-Dependent Allelic Imbalances in Human Bladder Tumors

Karen Koed,[1,3] Carsten Wiuf,[4] Lise-Lotte Christensen,[1] Friedrik P. Wikman,[1] Karsten Zieger,[1,2] Klaus Møller,[2] Hans von der Maase,[3] and Torben F. Ørntoft[1]

Molecular Diagnostic Laboratory, [1]Departments of Clinical Biochemistry, [2]Urology, and [3]Oncology, Aarhus University Hospital; and [4]Bioinformatics Research Center, Aarhus University, Aarhus, Denmark

Abstract

Bladder cancer is a common disease characterized by multiple recurrences and an invasive disease course in more than 10% of patients. It is of monoclonal or oligoclonal origin and genomic instability has been shown at certain loci. We used a 10,000 single nucleotide polymorphism (SNP) array with an average of 2,700 heterozygous SNPs to detect allelic imbalances (AI) in 37 microdissected bladder tumors from 17 patients. Eight tumors represented upstaging from Ta to T1, eight from T1 to T2+, and one from Ta to T2+. The AI was strongly stage-dependent as four chromosomal arms showed AI in > 50% of Ta samples, eight in T1, and twenty-two in T2+ samples. The tumors showed stage-dependent clonality as 61.3% of AIs were reconfirmed in later T1 tumors and 84.4% in muscle-invasive tumors. Novel unstable chromosomal areas were identified at chromosomes 6q, 10p, 16q, 20p, 20q, and 22q. The tumors separated into two distinct groups, highly stable tumors (all Ta tumors) and unstable tumors (2/3 muscle-invasive). All 11 unstable tumors had lost chromosome 17p areas and 90% chromosome 8 areas affecting *Netrin-1/UNC5D/MAP2K4* genes as well as others. AI was present at the *TP53* locus in 10 out of 11 unstable tumors, whereas 6 had homozygous *TP53* mutations. Tumor distribution pattern reflected AI as seven out of eight patients with additional upper urinary tract tumors had genomic stable bladder tumors ($P < 0.05$). These data show the power of high-resolution SNP arrays for defining clinically relevant AIs. (Cancer Res 2005; 65(1): 34-45)

Introduction

Bladder cancer is among the most prevalent cancers in the western world and is characterized by frequent recurrences. The disease is believed to be of monoclonal or oligoclonal origin and two different pathways have been suggested—one that is characterized by multiple papillomas over several years and one that is characterized by carcinoma *in situ* and often muscle-invasive disease at diagnosis. Studies using microsatellites, and more recently, array-based comparative genomic hybridization, have shown that loss of chromosome 9 is a frequent finding in the papillomatous disease course. A progressive genomic instability correlating to the stage of the disease has been described (1–4). In the case of noninvasive Ta transitional cell carcinomas, this includes loss of chromosome 9, or parts of it, as well as 1q+ and loss of the Y chromosome in males (2, 5). In invasive tumors, many alterations have been reported to be more or less common: 1p−, 2q−, 4q−, 5q−, 8p−, −9, 10q−, 11p−,11q−, 1q+, 2p+, 5p+, 8q+, 11q13+, 17q+, and 20q+ (2, 6–8). It has been suggested that these lost or gained regions harbor tumor suppressor genes and oncogenes, respectively. However, the large chromosomal areas involved often contain many genes, making meaningful predictions of the functional consequences of losses and gains very difficult. The recent introduction of single nucleotide polymorphism (SNP) arrays for scoring of allelic imbalance (AI) has increased the resolution—as has array-based comparative genomic hybridization (1, 3, 4). The high resolution can be used to pinpoint very narrow regions of losses and amplification, and makes it easier to define genes that may serve as tumor suppressors or oncogenes, thereby defining pathways that may be altered during tumor progression.

The SNP method has defined new regions of losses in invasive tumors at chromosome 6p (1), and has been shown to correlate well with microsatellite allelotyping (4). The previous works were based on SNP arrays with 1,500 SNPs. In the present paper, we used a 10,000 SNP array and this remarkable increase in resolution defined several novel chromosomes and chromosomal areas that are frequently subjected to imbalance in muscle-invasive bladder cancer such as 6q, 10p, 16q, 20p, 20q, and 22q. We use the term AI throughout the paper as we cannot rule out that conversion of a heterozygous SNP to a homozygous SNP is due to a high amplification of one allele. However, a recent report, as well as our own data, indicates that we almost exclusively detect losses (9).

The mechanism leading to genomic instability such as loss and gain of chromosomal material is poorly understood. In a recent publication, we could show a significant correlation between p53 inactivation and genomic instability. The previous finding was further substantiated in the present report, in which AI at the *TP53* locus was detected in almost all allelic unstable bladder tumors.

We used a material consisting of at least two tumors of different stages, and separated in time, from the same individual. We looked at AI related to disease course and at the recovery of AI from tumor to tumor. We found AI to be strongly related to stage and were able to define two separate groups of stable and unstable tumors. We identified the genes in three chromosomal areas showing common AI and found a possible influence of AI on the Netrin-1/UNC5 pathway.

Materials and Methods

Materials. Patients were selected from a prospective clinical data and tissue bank holding records on approximately 1,700 patients with bladder cancer. We selected at least two tumors of different stages from each patient, with the lowest stage as the first presented. The local scientific

Note: Supplementary information is available online at: http://www.mdl.dk.

Requests for reprints: Torben F. Ørntoft, Molecular Diagnostic Laboratory, Department of Clinical Biochemistry, Aarhus University Hospital, Skejby, DK-8200 Aarhus, Denmark. Phone: 45-894-95100; Fax: 45-894-96018; E-mail: orntoft@kba.sks.au.dk.

ethical committee approved the study. All patients gave informed consent and were granted anonymity. Tumors for DNA extraction were frozen immediately after surgery and stored at −80°C. Prior to DNA extraction, the tumors were transferred to Tissue-Tek (Sakura Finetek, Tokyo, Japan) and tumor tissue was crudely microdissected from tumor slices (20 μm thin). Germ line DNA was purified from blood from the same patient. Twelve of the tumors have previously been analyzed using a 1,500 SNP array, and six of these showed *TP53* mutations (1).

DNA Extraction. DNA was extracted from tumor tissue and blood using a Puregene protocol (Gentra Systems, Minneapolis, MN) according to the manufacturer's instructions. The DNA concentration was determined using a spectrophotometer, and diluted to a concentration of 50 ng/μL.

Single Primer Assay Protocol for GeneChip Mapping 10K Early Access Array. The Single Primer Assay Protocol (preparation of DNA target, labeling, hybridization to 10K GeneChip Early Access, washing and staining) was done according to the manufacturer's instructions (Affymetrix, Santa Clara, CA, described in ref. 10). In short, 250 ng of genomic or tumor DNA was digested with 10 units of *Xba*I. The 4-bp *Xba*I overhangs were ligated (T4DNA Ligase) to an Adaptor Xba fragment. A PCR reaction was set up with a PCR primer complementary to the Adaptor Xba fragment (PCR primer Xba). For each sample, four to five reactions were needed. The PCR products were purified according to the Qiagen manual (QIAquick PCR Purification Kit Protocol, Qiagen, Darmstadt, Germany) except that all DNA elutes from the four to five PCR reactions were collected in one tube. Purified PCR product (20 μg) was fragmentized with DNase. The fragmented DNA was then end-labeled by biotinylated-ddATP in the presence of ~30 units of Terminal Transferase (TdT). The labeled DNA was hybridized to the 10K chip overnight. After removal of the hybridization cocktail, the chip was stained with streptavidin for 45 minutes, then with biotinylated anti-streptavidin for 10 minutes, and then with streptavidin-R-phycoerythrin conjugate, for 20 minutes. The chips were scanned using an HP scanner (Hewlett-Packard, Palo Alto, CA, USA) according to the manufacturer's recommended conditions (HuSNP Mapping Assay Manual, Affymetrix P/N 700308). Hybridization signal was detected by Affymetrix Microarray Suite 5.0 software (Affymetrix). Genotype calls were generated using the Genotyping Tools software.

Sequencing of *TP53*. Exons 5, 6, 7, and 8 of the *TP53* gene were sequenced in both directions. Fragments representing each exon and the adjacent intron-exon boundaries were generated by PCR. The primers were as follows: *TP53* exons 5 and 6 sense, 5′-CTTGTGCCCTGACTTTCAACTCTGTCTC-3′ and antisense, 5′-GGGTCTCTGGGAGGAGGGGTTAAG-3′; *TP53* exon 7 sense, 5′-CAGGTCTCCCCAAGGCGCACTG-3′ and antisense, 5′-CTCTGCTTGCCGCTGACCCCTG-3′; *TP53* exon 8 sense, 5′-GTAGGACCTGATTTCCTTACTGCCTCTTGC-3′ and antisense, 5′-GCGGTGGAGGAGACCAAGGGTGCAGTTAT-3′. The PCR fragments were sequenced using the BigDye Terminator Kit (Applied Biosystems, Foster City, CA) and the ABI 3100 genetic analyzer (Applied Biosystems). The sense and antisense primers used for generation of the PCR fragments were also used for sequencing of the sense and antisense strands. The obtained sequences were compared with *TP53* sequences from Genbank.

Microsatellite Instability Analysis. The microsatellite stability status of the tumors was determined by comparing somatic alterations in the length of mononucleotide repeat sequences between germ line DNA and tumor DNA according to the method characterized by Suraweera and coworkers (11). Five mononucleotide repeat sequences were coamplified in a multiplex PCR according to the method described. The mononucleotide markers used were BAT-25, BAT-26, NR-21, NR-22, and NR-24. The PCR products were separated on an ABI PRISM 3100 and GeneScan 3.7 software was used to calculate the size of each fluorescent PCR product.

Single Nucleotide Polymorphism and Gene Position. Both the SNPs and the genes were positioned according to the same genome build. The genome build used was: UCSC Genome Browser http://genome.ucsc.edu/ April 2003 assembly. The April 2003 human reference sequence (UCSC version hg15) is based on NCBI Build 33.

Algorithm for Allelic Imbalance Scoring. We developed an algorithm based on a Hidden Markov Model to score AI. The Hidden Markov Model has two hidden (unobserved) states, Loss and No-loss. For each tumor and SNP, a state is assigned based on a probability model. The Hidden Markov Model jumps between the two states with probabilities that depend on the state of the previous SNP (12, 13). When in the Loss state, the SNP cannot be heterozygous in tumor; when in the No-loss state, the SNP cannot be scored as homozygous in tumor, while being heterozygous in blood. We used the EM-algorithm to optimize the model. For further details, see the supplementary material.

Results

Scoring of Allelic Imbalance. The GeneChip Mapping 10K Early Access array from Affymetrix was used to examine AI by comparing the SNP pattern in DNA from microdissected bladder tumor cells to DNA from normal blood leukocytes. The material examined was selected in a tissue bank with clinical follow-up. A total of 17 patients that showed stage progression were included, and from each of these, two or three tumors were available for microdissection (Table 1). We obtained two tumors from 14 patients (five progressing from noninvasive Ta to T1, eight from superficially invasive T1 to muscle-invasive T2-4, and one from Ta to T2-4), and three tumors from 3 patients (two noninvasive Ta and an invasive T1).

Conversion of a heterozygous SNP in normal blood cells to a homozygous SNP in tumor tissue indicates an AI that can be due to loss of one allele, an amplification of the other allele or an analytic error. We compared the frequency of retained or lost heterozygosity in blood and tumor cells and found only one SNP out of approximately 2,000 converted from heterozygous in tumor to homozygous in blood, whereas the reverse, AI in tumor compared with blood was observed in 217 cases (Table 2*A*). That AI only occurred in tumors indicates a highly reproducible performance of the analysis.

When the software used to calculate the SNP call was unable to decide on the call (AA, BB, AB) the SNP was scored as a No Call. The frequency of No Calls was much higher in tumor tissue (474-800) than in blood cells (317), indicating either a contamination of tumor cells having AI with DNA from normal cells infiltrating the tumor, a mixture of tumor cells, some having AI at that particular locus, or partial or complete loss of both alleles such as in homozygous deletions (Table 2*A*). Loss of both alleles, homozygous deletions, seemed to be rare as the number of Homozygous to No Call changes was the same in blood and tumor tissue (1%; Table 2*A*).

Because No Calls were much more common in areas where AI was detected, we hypothesized that normal tissue contamination could be the major factor and developed an algorithm that scored the presence of AI based on both converted SNPs and No Call SNPs. The algorithm scores a No Call as AI when the genomic distance is closest to a converted SNP (heterozygous in blood, homozygous in tumor) and scores a No Call as retention (no AI) when closest to a retained, heterozygous SNP. This algorithm was used throughout the study. The total number of SNPs on the array was 8,686 and the number of SNPs the software was able to give a call as heterozygous or homozygous (call rate) was 96% in blood decreasing in tumor tissue with increasing stage until stage T2-4, which showed a call rate of 91% (Table 2).

Allelic Imbalance in Relation to Tumor Stage. We analyzed the AI in relation to chromosomal location of the SNPs and tumor stage (Table 3). In stage Ta tumors, we discovered frequent AI as expected at 9q (66.7%), a little less in 9p (41.7%), and also frequent AI at 20p as well as q (both 75%) and at 18q (50%). As seen from the table, an average of 113 SNPs per Ta tumor showed AI at 9q amounting to 52% of all SNPs. These SNPs cover 36.4 Mb or almost

Table 1. Clinical data on tumors, level of AI in total and at the *TP53*, *UNC5D*, and *NTN1* loci, as well as results from sequencing of *TP53*

Patient ID-visit number	UTT	Time between tumors (mo)	Tumor		AI (high/low)	*TP53*		*UNC5D*	*NTN1*
			Stage	Grade		AI	Mutation	AI	AI
112-2			Ta (3)	low	+	−		+	
112-12	+	47	T1 (3)	low	+	−	+	+	
747-3			Ta (2)	low		−			
747-5	+	7	T1 (3)	low		−			
825-3			Ta (3)	low		−			
825-5	+	6	T1 (3)	low		−			
865-1			Ta (2)	low	+	−	+	+	
865-2	+	5	T1 (2)	low		−			
1058-3			Ta (2)	low		−			
1058-10	+	29	T1 (3)	high	+	G→A 853 (homozygous mutation)*	+	+	
140-8			Ta (3)	low		−			
140-12		18	Ta (3)	low		−			
140-16	+	15	T1 (3)	low		−		+	
154-5			Ta (2)	low		−			
154-6		10	Ta (2)	low		−			
154-10		31	T1 (3)	high	+	−	(+) †	+	
166-5			Ta (2)	low		−			
166-9		25	Ta (2)	low		−			
166-14	+	24	T1 (3)	low		−			
941-4			Ta (3)	low		−			
941-6	+	10	T2-4 (3)	low		−			
172-3			T1 (3)	low		−			
172-4		5	T2-4 (3)	low		−			
365-1			T1 (3)	low		−			
365-3		7	T1/T2-4 (3)	low		−			
501-1			T1 (3)	low		−			
501-5		26	T2-4 (3)	high	+	−		+	
839-1			T1 (3)	high	+	Del C 482 (homozygous mutation) ‡	+	+	
839-2		12	T2-4 (3)	high	+	Del C 482 (homozygous mutation) ‡	+	+	
1013-1			T1 (3)	low		GC→TT 919 (heterozygous mutation)§			
1013-3		9	T2-4 (3)	high	+	GC→TT 919 (homozygous mutation)§	(+) †	+	
1017-1			T1 (3)	low		−	+		
1017-3		9	T2-4 (3)	high	?	−	+	+	
1033-1			T1 (3)	high	+	G→C 396 (homozygous mutation)‖	+	+	
1033-2		6	T2-4 (3)	high	+	G→C 396 (homozygous mutation)‖	+	+	
1276-1			T1 (3)	high	+	−	+	+	
1276-3		7	T1/T2 (3)	high	+	−	+	+	

Abbreviations: Ho, mutation of nucleotide 853 of the *TP53* coding sequence ($Glu^{285}Lys$).
*G→A mutation of nucleotide 853 of the *TP53* coding sequence ($Glu^{285}Lys$).
† (+) AI occurred very close to the *UNC5D* gene.
‡ Deletion of C at nucleotide 482 of the *TP53* coding sequence (stop codon at position 169 of the p53 amino acid sequence).
§GC→TT mutation of nucleotide 919 of the *TP53* coding sequence ($Ala^{307}Ser$, splice mutation).
‖G→C mutation of nucleotide 396 of the *TP53* coding sequence ($Lys^{132}Arg$).

54% of 9q. In stage T1 tumors more chromosomes were frequently involved in AI such as 2q, 8p, 9p, 9q, 10q, 11q, 20p, and 20q. Regarding 2q, the number of SNPs showing AI was increased from 0.4 per Ta tumor to 45.5 per T1 tumor. In stage T2-4 tumors, additional areas showed frequent AI such as 1q, 3p, 4q, 5q, 6p, 6q, 10p, 11p, 12q, 13q, 14q, 16q, 17p, and 22q. Remarkably stable regions were 16p, 17q, and 19p. The latter only showed loss of one SNP in 1 tumor out of all 37 tumors examined. This might indicate that chromosome 19 harbors genes that are essential for cellular survival, or is resistant to imbalances. The extent of the AI varied in T2-4 tumors from narrow chromosomal areas as in 10p and 12q, where only 4 and 10 Mb were involved, respectively, to much larger

areas as for example 34.8 Mb at 9q (51%), 26 Mb of 6p (44.6%), and 8.3 Mb (43%) of 17p.

Allelic Imbalance Repeated in Subsequent Tumors from the Same Patient. Our material consisted of more than one tumor from each patient, thus making it possible to compare the extent and location of AI conserved between the two. As bladder cancer is regarded as a monoclonal or oligoclonal disease one would expect that AIs would be repeated in later tumors together with newly acquired AI. We found Ta and T1 tumors to be significantly more different (t test, $P < 0.05$) than T1 and T2+ tumors (Table 2*C*). Stage Ta and T1 tumors had an average of 61.3% AIs in common, whereas T1 and T2+ tumors had 84.4%. In the two cases where none and all

Table 2. Calls and Clonality of SNPs

(A) Comparison of the heterozygous and homozygous calls in blood and tumor tissue

	Blood		
Tumor	Heterozygous SNPs	Homozygous SNPs	No Call
Heterozygous SNPs	2,113 (24%)	1 (0%)	83 (1%)
Homozygous SNPs	217 (2%)	5,583 (64%)	61 (1%)
No Calls	396 (5%)	63 (1%)	170 (2%)

(B) Summary of the genotype calls in blood and tumor tissue

	Blood	Ta	T1 (Ta)*	T1 (T2-4)†	T2-4
Heterozygous SNPs	2,721 (31%)	2,520 (29%)	2,114 (24%)	2,197 (25%)	1,829 (21%)
Homozygous SNPs	5,648 (65%)	5,692 (66%)	5,921 (68%)	5,836 (68%)	6,057 (70%)
No Call	317 (4%)	474 (5%)	651 (7%)	653 (7%)	800 (9%)

(C) The fraction of AI that is repeated in later tumors from the same patient

Patient id	Tumor	Tumor 1 (Ta)→3 (T1)	Tumor 1 (Ta)→2 (Ta)
	Ta→T1		
166	0.74	0.46	0.37
154	0.4	0.5	0.5
140	0.86	0.89	0.07
112	0.64	—‡	—
747	0.35	—	—
825	0.97	—	—
865	0.51	—	—
1058	0.43	—	—
	Ta→T2		
941	0	—	—
	T1→T2		
172	0.56	—	—
365	0.99	—	—
501	0.98	—	—
839	0.69	—	—
1013	0.94	—	—
1017	1	—	—
1033	0.77	—	—
1276	0.82	—	—

NOTE: B, The results are given as an average and in percentage. In total, 8,686 SNPs were investigated. Call rates: blood, 96%; Ta, 95%; T1 (Ta), 93%; T1 (T2-4), 93%; T2-4, 91%.
*T1 (Ta), T1 tumors where the previous tumor identified in the same patient was a Ta tumor.
†T1 (T2-4), T1 tumors where the subsequent tumor from the same patient was a T2-4 tumor.
‡(—) Only two tumors were analyzed from these patients.

Table 3. AI in relation to chromosomal arm and stage of bladder cancer (Ta, T1, T2-4)

	Ta (*N* = 12)			T1 (*N* = 16)			T2-4 (*N* = 9)		
	Amount of tumors with AI	Number of SNPs with AI	Mb of AI	Amount of tumors with AI	Number of SNPs with AI	Mb of AI	Amount of tumors with AI	Number of SNPs with AI	Mb of AI
1 p	1 (8.3)*	7 (0.2)*	2.28 (0.2)*	*6 (37.5)**	326 (5.9)*	0.92 (5.0)*	*4 (44.4)**	361 (11.7)*	1.15 (11.1)*
q	*5 (41.7)**	291 (8.0)*	0.94 (7.8)*	*7 (43.8)**	802 (16.5)*	2.42 (15.1)*	**7 (77.8)***	432 (15.8)*	1.34 (14.8)*
2 p	0 (0.0)*	0 (0.0)*	0 (0.0)*	3 (18.8)*	264 (5.3)*	6.95 (4.9)*	2 (22.2)*	531 (19.0)*	1.41 (17.7)*
q	*3 (25.0)**	5 (0.1)*	0.07 (0.0)*	**10 (62.5)***	726 (10.8)*	2.20 (9.8)*	**7 (77.8)***	*1102 (29.2)**	*3.59 (28.4)**
3 p	0 (0.0)*	0 (0.0)*	0 (0.0)*	*4 (25.0)**	365 (7.4)*	1.01 (7.2)*	**6 (66.7)***	468 (16.8)*	1.45 (18.3)*
q	2 (16.7)*	222 (5.8)*	7.16 (5.7)*	*5 (31.3)**	534 (10.5)*	1.72 (10.3)*	*4 (44.4)**	324 (11.3)*	1.04 (11.1)*
4 p	1 (8.3)*	1 (0.1)*	0 (0.0)*	*4 (25.0)**	302 (11.6)*	7.13 (9.6)*	*4 (44.4)**	185 (12.6)*	4.76 (11.3)*
q	2 (16.7)*	137 (2.7)*	3.65 (2.2)*	*5 (31.3)**	601 (8.9)*	1.76 (7.9)*	**5 (55.6)***	388 (10.2)*	1.12 (9.0)*
5 p	2 (16.7)*	7 (0.4)*	0.41 (0.1)*	2 (12.5)*	31 (1.3)*	5.34 (0.8)*	*4 (44.4)**	233 (16.7)*	6.31 (15.9)*
q	*3 (25.0)**	7 (0.1)*	0.94 (0.1)*	*4 (25.0)**	1101 (14.9)*	3.07 (15.0)*	**7 (77.8)***	*1100 (26.4)**	*3.00 (26.0)**
6 p	2 (16.7)*	187 (6.5)*	4.53 (6.5)*	*4 (25.0)**	646 (16.8)*	1.57 (16.8)*	**6 (66.7)***	*972 (45.0)**	*2.35 (44.6)**
q	1 (8.3)*	2 (0.0)*	0 (0.0)*	*4 (25.0)**	483 (8.1)*	1.33 (7.9)*	**7 (77.8)***	*1305 (38.9)**	*3.67 (38.6)**
7 p	1 (8.3)*	72 (3.2)*	2.29 (3.4)*	2 (12.5)*	226 (7.6)*	6.69 (7.5)*	2 (22.2)*	2 (0.1)*	0 (0.0)*
q	1 (8.3)*	47 (1.5)*	2.01 (1.7)*	2 (12.5)*	264 (6.3)*	9.69 (6.3)*	2 (22.2)*	100 (4.3)*	3.35 (3.8)*
8 p	2 (16.7)*	69 (3.8)*	1.73 (3.5)*	**8 (50.0)***	*947 (39.2)**	*2.45 (36.9)**	**6 (66.7)***	*621 (45.7)**	*1.62 (43.3)**
q	*3 (25.0)**	35 (1.0)*	1.19 (1.0)*	*6 (37.5)**	879 (18.7)*	2.66 (17.6)*	*3 (33.3)**	373 (14.1)*	1.15 (13.5)*
9 p	*5 (41.7)**	*762 (30.2)**	*1.38 (30.3)**	**11 (68.8)***	*1221 (36.3)**	*2.14 (35.2)**	**7 (77.8)***	*549 (29.0)**	*9.58 (28.0)**
q	**8 (66.7)***	**1355 (52.0)***	**4.38 (53.8)***	**10 (62.5)***	*1711 (49.3)**	*5.39 (49.6)**	**6 (66.7)***	**1026 (52.5)***	**3.13 (51.3)***
10 p	*3 (25.0)**	15 (0.8)*	0.97 (0.2)*	*5 (31.3)**	299 (12.6)*	7.58 (12.7)*	**5 (55.6)***	158 (11.9)*	3.79 (11.3)*
q	*5 (41.7)**	36 (0.9)*	8.06 (0.7)*	**9 (56.3)***	941 (17.5)*	2.39 (16.5)*	**7 (77.8)***	522 (17.2)*	1.22 (15.0)*
11 p	*4 (33.3)**	163 (6.9)*	0.37 (6.2)*	*7 (43.8)**	996 (31.8)*	2.44 (30.9)*	**5 (55.6)***	*773 (43.8)**	*1.88 (42.2)**
q	*5 (41.7)**	274 (7.4)*	5.08 (5.4)*	**8 (50.0)***	962 (19.4)*	2.29 (18.1)*	**6 (66.7)***	518 (18.6)*	1.24 (17.5)*
12 p	1 (8.3)*	2 (0.2)*	0.10 (0.0)*	3 (18.8)*	89 (6.4)*	3.31 (6.1)*	*4 (44.4)**	86 (11.0)*	3.07 (10.1)*
q	1 (8.3)*	64 (1.7)*	1.46 (1.3)*	3 (18.8)*	164 (3.2)*	0.45 (3.0)*	**5 (55.6)***	348 (12.0)*	9.49 (11.2)*
13 p	–	–	–	–	–	–	–	–	–
q	*4 (33.3)**	326 (7.1)*	8.22 (7.3)*	*6 (37.5)**	922 (15.2)*	2.28 (15.1)*	**7 (77.8)***	*1102 (32.2)**	*2.71 (32.0)**
14 p	–	–	–	–	–	–	–	–	–
q	2 (16.7)*	50 (1.3)*	1.50 (1.4)*	*5 (31.3)**	402 (8.0)*	1.14 (8.2)*	**5 (55.6)***	675 (23.7)*	1.86 (23.8)*
15 p	–	–	–	–	–	–	–	–	–
q	*4 (33.3)**	23 (0.7)*	7.12 (0.7)*	*6 (37.5)**	479 (11.6)*	1.43 (11.1)*	*4 (44.4)**	478 (20.7)*	1.47 (20.4)*
16 p	1 (8.3)*	2 (0.3)*	0.15 (0.0)*	3 (18.8)*	79 (8.5)*	3.40 (7.9)*	1 (11.1)*	45 (8.6)*	1.78 (7.4)*
q	1 (8.3)*	2 (0.1)*	0.02 (0.0)*	3 (18.8)*	197 (9.3)*	6.20 (9.4)*	**5 (55.6)***	159 (13.3)*	4.69 (12.7)*
17 p	*3 (25.0)**	104 (15.5)*	3.06 (13.3)*	*7 (43.8)**	*348 (38.8)**	*1.04 (33.8)**	**6 (66.7)***	*250 (49.6)**	*7.43 (43.0)**
q	1 (8.3)*	6 (0.5)*	3.36 (0.5)*	2 (12.5)*	157 (10.6)*	9.75 (11.3)*	1 (11.1)*	40 (4.8)*	2.04 (4.2)*
18 P	2 (16.7)*	65 (8.6)*	1.23 (8.3)*	*6 (37.5)**	*279 (27.7)**	*5.53 (28.1)**	2 (22.2)*	69 (12.2)*	1.39 (12.5)*
q	**6 (50.0)***	249 (10.7)*	6.86 (9.8)*	*6 (37.5)**	*796 (25.6)**	*2.39 (25.6)**	*4 (44.4)**	*529 (30.3)**	*1.56 (29.6)**
19 P	0 (0.0)*	0 (0.0)*	0 (0.0)*	1 (6.3)*	1 (0.4)*	0 (0.0)*	0 (0.0)*	0 (0.0)*	0 (0.0)*
q	0 (0.0)*	0 (0.0)*	0 (0.0)*	3 (18.8)*	77 (7.6)*	4.20 (8.9)*	2 (22.2)*	68 (12.0)*	3.42 (12.9)*

(Continued on the following page)

Table 3. AI in relation to chromosomal arm and stage of bladder cancer (Ta, T1, T2-4) (Cont'd)

	Ta (*N* = 12)			T1 (*N* = 16)			T2-4 (*N* = 9)		
	Amount of tumors with AI	Number of SNPs with AI	Mb of AI	Amount of tumors with AI	Number of SNPs with AI	Mb of AI	Amount of tumors with AI	Number of SNPs with AI	Mb of AI
20 p	9 (75.0)*	35 (3.2)*	2.00 (0.7)*	9 (56.3)*	120 (8.2)*	2.69 (6.7)*	5 (55.6)*	125 (15.3)*	2.95 (13.1)*
q	**9 (75.0)***	31 (3.5)*	3.14 (0.8)*	**9 (56.3)***	53 (4.5)*	1.22 (2.4)*	**6 (66.7)***	140 (21.0)*	5.03 (17.5)*
21 p	–	–	–	–	–	–	–	–	–
q	1 (8.3)*	147 (8.3)*	0.33 (8.3)*	*7 (43.8)**	409 (17.4)*	9.10 (17.1)*	2 (22.2)*	151 (11.4)*	3.45 (11.5)*
22 p	–	–	–	–	–	–	–	–	–
q	0 (0.0)*	0 (0.0)*	0 (0.0)*	2 (12.5)*	22 (2.3)*	1.44 (2.7)*	**7 (77.8)***	*154 (29.0)**	*9.58 (31.4)**

*Percentage. Chromosomal arms showing more than 25% AI of SNPs are shown in italics and those showing more than 50% AI in boldface. (–) No SNPs on p arm.

alterations were in common between the two tumors, this was due to the presence of very few alterations in the first tumor. We did hierarchical clustering on the tumors based on their shared AI pattern. A cluster dendrogram of this distance shows how pairs of tumors from the same patient in several cases cluster together based on common AI, and that tumors occur in two groups related to the number of AIs (Fig. 1*A*).

Two Distinct Groups of Tumors with High and Low Allelic Stability. To analyze the distribution of AIs on tumor stages, we plotted the SNPs having AI against those having retained heterozygosity. The tumors fell on a straight line but with a distinct separation into a group of tumors with a high instability of the genome, and a group with a low instability. The group of genetically stable tumors correlated with lower stage: Ta (12/12), T1 (10/16), and T2+ (3/9), whereas the group of genetically unstable tumors correlated with higher stage: Ta (0/12), T1 (6/16), and T2+ (6/9; $P < 0.05$, χ^2; Fig. 1*B*). Our AI scoring method includes SNPs that are converted from heterozygosity to homozygosity as well as SNPs that are scored as No Calls in tumors, although being heterozygous in blood. Fitting a straight line indicates that the No Calls are correctly interpreted as reduced to homozygosity in the majority of cases (Fig. 1*C*). There was a good correlation (0.72, $P < 0.01$) between the total number of SNPs showing AI and the number of chromosomal regions that were affected by AI. However, some scattering of tumors, especially stage T2+, was detected as some had a relatively low number of SNPs showing AI but with many regions affected (Fig. 1*D*).

The presence of high or low AI showed an interesting correlation to the organ distribution of the tumors. Eight patients had a generalized urothelial syndrome with upper urinary tract tumors (UTT) in addition to the bladder tumors (Table 1). Seven of these eight patients belonged to the group of nine patients with low AI in both tumors, and only one belonged to the group of eight patients having high AI ($P < 0.05$). This can be related to findings in the colon where proximal tumors in the cecum are less chromosomally unstable than tumors in the distal colon. In contrast, the proximal tumors have more pronounced microsatellite instability. Thus, we wanted to determine whether the higher incidence of chromosomally stable bladder tumors in the patients with UTT likewise could signify a higher frequency of microsatellite instability. We therefore tested the presence of microsatellite instability in the stable tumors with UTT using a panel of five mononucleotide repeats that shows high sensitivity in characterizing high microsatellite instability, low microsatellite instability, or microsatellite-stable colorectal cancer (11). All the tested tumors were microsatellite stable in all five loci (data not shown) and no microsatellite instability could be detected. This correlates well with recent publications (14–16).

Regions of Common Losses in the Chromosomal Stable and Unstable Group. In the group with a low level of AI, only chromosome 9 was frequently involved in common losses, 30% to 60% of the samples had lost parts of chromosome 9 (Fig. 2*A*, *blue dots*). The AI of chromosome 9 was equally distributed on the three stages. In the unstable group, a similar amount of chromosome 9 AIs were detected as in the stable group, amounting to six out of nine T1 and T2+ tumors (Fig. 2*A*, *red dots*).

In the unstable group, some chromosomal areas were very frequently involved. All unstable tumors had lost a region on chromosome 17p close to the *TP53* locus and 10 out of 11 had lost two regions on chromosome 8p (Fig. 2*A*, *red dots*). Other frequently involved chromosomal regions are listed in Table 4, with an indication of genes that are of tumor biological interest in these regions.

We took a closer look at the three regions where 90% or more of the unstable tumors had AI, the two regions at chromosome 8p (6.1-13.8 and 31.3-36.6 Mb) and the one region at chromosome 17p (0.9-12.6 Mb; Fig. 2*B*). In the first 8p region (6.1-13.8 Mb), all unstable tumors, except 501-5, showed AI as well as three of the stable tumors (Fig. 2*B*). In the second 8p region (31.3-36.6 Mb), all unstable tumors, except 501-5, showed AI as well as four of the stable tumors (Fig. 2*B*).

At chromosome 17, all tumors had AI in a region immediately next to the tumor suppressor *TP53*, and from 0.9 to 12.6 Mb, all unstable tumors, except 1017-3 (T2-4), showed AI (Fig. 2*B*). Patient 1017 has germ line homozygous SNPs in the region from 5.8 to 8.5 Mb (eight SNPs), so we were not able to detect AI in this region. The areas were scrutinized for genes of interest in relation to cancer and we found several genes that could be either putative tumor suppressors, or had a function that would

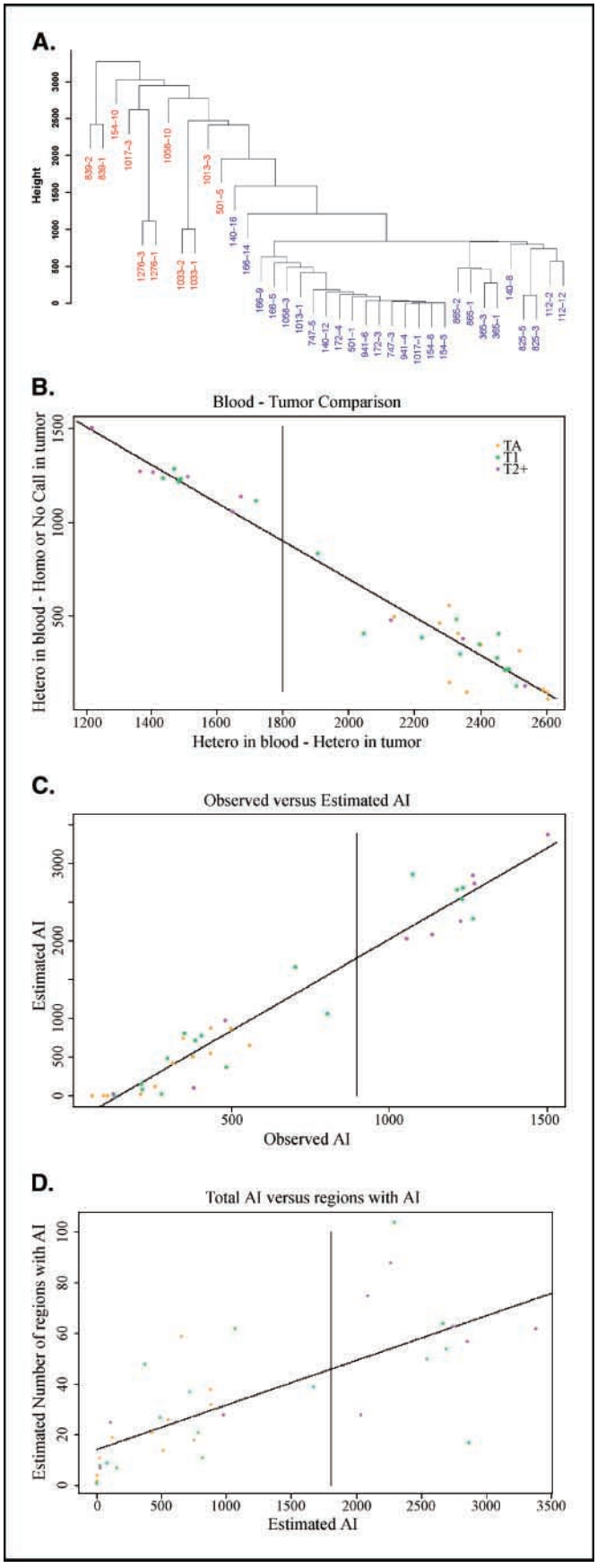

benefit the malignant process if down-regulated or abandoned (Fig. 2*B*).

It was interesting that *Netrin-1* (*NTN1*) on chromosome 17 showed AI in all unstable tumors, and that *UNC5D* on chromosome 8 showed AI in all except one, 501-5 (Fig. 2*B* and Table 1). These two molecules form ligand and receptor. At the gene expression level *Netrin-1* is unchanged in tumor tissue, but some members of the *UNC5* family are down-regulated in bladder cancer in a stage-related and grade-related way (see Fig. 1 in supplementary material). Screening for mutations in *UNC5D* and *Netrin-1* is ongoing and the tumors examined have thus far confirmed loss of heterozygosity based on polymorphisms, however, no inactivating mutations have been detected in the sequenced exons.

Relation Between Genomic Instability and p53 Inactivation. In a previous publication, we found a relation between p53 inactivation and genomic instability in bladder tumors (1). We therefore sequenced *TP53* on microdissected tumor tissue from all tumors of which tumors from six patients were included in the previous publication. We reconfirmed our previous finding of homozygous mutations in five tumors and a heterozygous mutation in one tumor (Table 1). Furthermore, we discovered a new homozygous *TP53* mutation (patient 1058-10).

The fine mapping of possible AI with the 10,000 SNP array confirmed that there was AI at the *TP53* locus explaining the homozygous sequence. Furthermore, it was striking that all 11 unstable tumors except one (which had germ line homozygous SNPs in the region as earlier mentioned) had AI at the *TP53* locus (Table 1). Thus, inactivating events other than mutation may have hit the remaining allele.

Discussion

We used a 10,000 SNP array from Affymetrix to detect AIs in a set of 37 bladder tumors from 17 patients. We microdissected tumor DNA and compared this to normal leukocyte DNA, and were on average able to obtain information from approximately 2,700 SNPs distributed along the chromosomes with the same density as coding genes.

The SNP array assay was working with a call rate > 90%, however, the number of No Calls where the software could not identify the SNP call was much increased in tumor tissue compared with normal tissue. As this reduced the informative SNPs, we decided to build an algorithm that scored the No Calls as being homozygous if they occurred together with SNPs that had converted from heterozygous to homozygous. In this way, we obtained continuous stretches of AIs.

The SNP array method has been compared extensively to microsatellite analysis and a good correlation was detected (1, 4, 9, 10).

Figure 1. *A,* cluster dendrogram (using Average-Linkage) based on the similarity of SNP losses. The stable and unstable tumors, respectively, cluster together, and two or three tumors from the same patient are close in the majority of cases. *Red,* the unstable group of tumors; *blue,* the stable group. Labels refer to patient identification number in Table 1. *B,* the relationship between the number of SNPs scored as heterozygous in blood despite being homozygous or No Call in tumor, and the number of SNPs with retained heterozygosity. There are two distinct groups, the stable group and the unstable group. *Vertical line,* point of separation. *C,* observed AI (here converted heterozygous or heterozygous scored as No Calls in tumor) and estimated AI. If observed AI is small, estimated AI is sometimes even smaller because (i) our AI scoring method underestimates AI when only few converted heterozygous are present and (ii) observed AI includes No Calls that are not AI (see Table 2). *D,* estimated AI in relation to the number of regions with AI. There is significant correlation between these two (0.72, $P < 0.05$).

Table 4. Chromosomal regions, which are commonly lost in unstable bladder tumors according to chromosomal location and with the identification of genes of potential tumor biological interest

Chromosome	Position in Mb		Genes of tumor biological interest in the region
	≥50%	≥70%	
2q	173-177		*ATF2* (1386*), *CHN1* (1123)
	212-214		–
5q	62-63		–
	118-125		*GG2-1* (25816), *LOX* (4015)
	134-160		*CTNNA1* (1495), *NRG2* (9542)
	169-175	**171.2**	***STK10*** (6793), ***FBXW1B*** (23291)
6p	0.2-21	**16-21**	***ID4*** (3400)
	26-45		*MAPK14* (1432), *MDC1* (9656), *SPDEF* (25803), *UNC5CL* (222643), *PARC* (23113), *P21* (1026), *BAK1* (578)
	46-48		*TNFRSF21* (27242)
6q	135-168		*MAP3K5* (4217), *PIGPC1* (64065), *WTAP* (9589), *MAP3K4* (4216)
8p	1-47	**2-40**	Whole of chr8p (see ref. 37) and Fig. 2*B*, ***sFRP1*** (6422)
8q	63-76		*Pin2/TRF* (7013)
	134-142		*CHRAC1* (54108)
9q	95-97		*TMEFF1* (8577)
	99-131		*SMC2L1* (10592), *RAD23B* (5887), *KLF4* (9314), *AMBP* (259), *TNFS15* (9966), *DEC1* (50514), *TNFSF8* (944), *DBC1* (1620), *TRAF1* (7185), *CEP1* (11064), *PTGES* (9536), *DDX31* (64794), *TSC1* (7241)
10q	49-68	**50-52**	*MAPK8 (5599), ERCC6 (2074),* ***MRIP2*** *(119016),* ***MSMB*** (4477), *DKK1* (22943), *UBE2D1* (7321)
	130-133		*MGMT* (4255)
11p	2-21		*#PHEMX* (10077), *#TSSC4* (10078), *#CDKN1C* (1028), *#TSSC3* (7262), *#NUP98* (4928), *#RRMI* (6240), *ST5* (6764), *WEE1* (7465), *DKK3* (27122), *PI3KC2A* (5286), *TSG101* (7251), *HTATIP2* (10553)
	22-25		*FANCF* (2188), *GAS2* (2620)
	26-43		*WT1* (7490), *WIT-1* (51352), *TRAF6* (7189), *RAG1* (5896)
	44-46		*KAI1* (3732)
13q	42-56		*RB1* (5925), *TSC22* (8848), RFP2 (10206), *KCNRG* (283518), *DLEU1* (10301), *DLEU2* (8847), *FAM10A4* (145165), *DDX26* (26512)
	100-102		
17p	0.9-16	0.9-15	*TP53* (7157), (see Fig. 2B), *ADORA2B* (136)
18p+q	10-29		*CIDEA* (1149), *PTPN2* (5771)
	44-77		*MADH2* (4087), *SMAD7* (4092), *SMAD4* (4089), *MBD1* (4152), *MBD2* (8932), *CGBP* (30827), *DCC* (1630), *POLI* (11201), *MASPIN* (5268), *CDH7* (1005), *CDH19* (28513), *DNAM-1* (10666)

NOTE: Regions, as well as genes within these, which show more than 70% AI are shown in boldface. Potential tumor suppressor genes in an imprinted region on chr11 (telomere-4 Mb).
*ID in LokusLink

The present method for the 10,000 SNP array is a modification of the method used for the 1,500 SNP array as the latter was based on multiplex PCR with different PCR primers. The present method uses a random *Xba*I cleavage and a ligase reaction followed by a homogenous PCR. With this method, we cannot exclude that the remaining allele is being duplicated as we only score the nucleotide composition at the SNP locus, not the level of each nucleotide. There are attempts to construct algorithms that will detect gain of an allele based on SNP arrays, but these still need optimization and verification. We believe that the AIs

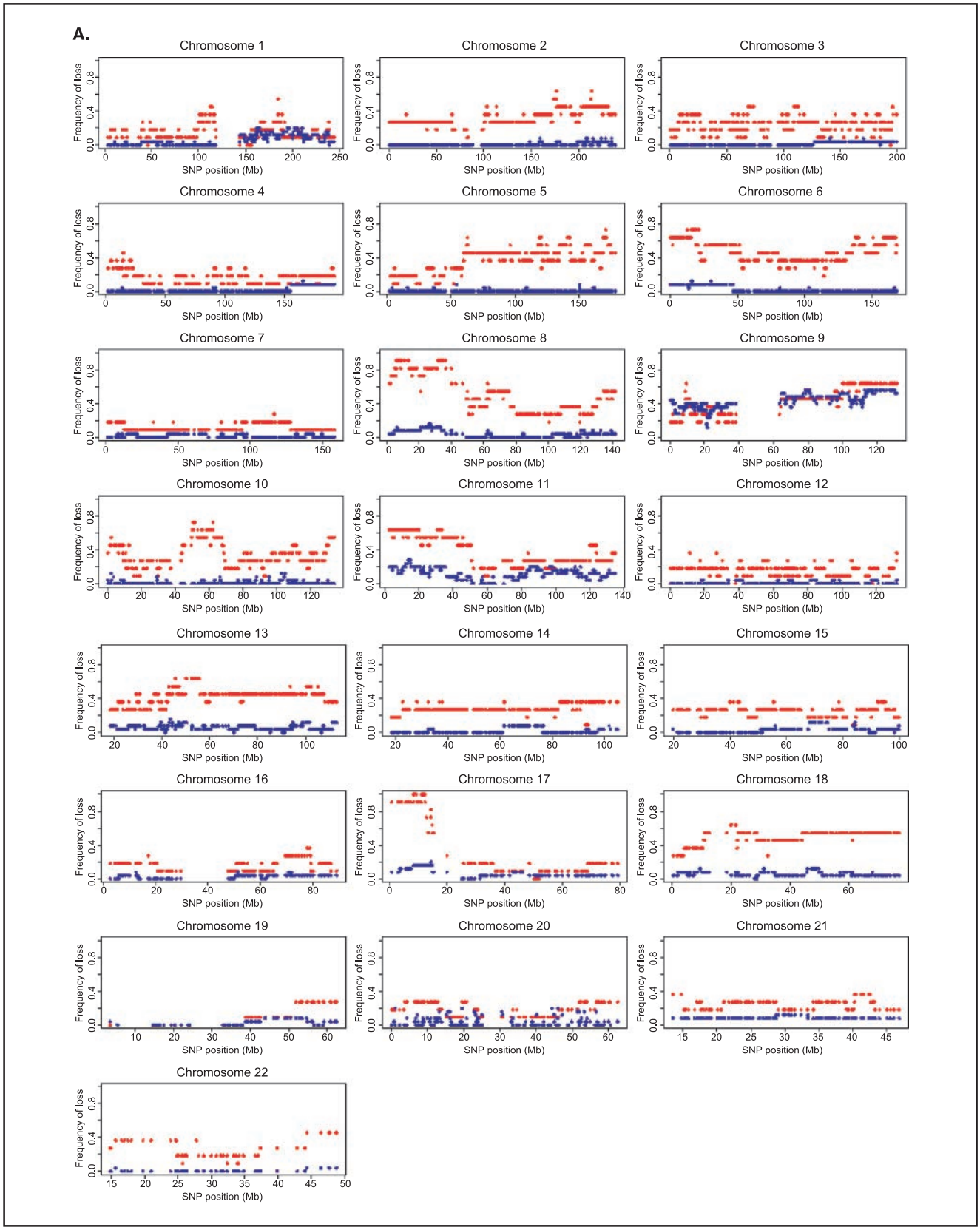

Figure 2. *A,* frequency of AI in the group of tumors with a high imbalance (*red dots*) and the group with low imbalance (*blue dots*). For each chromosome, one SNP is shown as a dot. *B,* close-up of chromosomes 8 and 17. Loss of chromosomal region/AI is represented with a vertical line. All unstable tumors are indicated (*boldface* and *red*). All unstable tumors except 501 $T_{2\text{-}4}$ have lost both areas on chromosome 8 and 17. 501 $T_{2\text{-}4}$ have only lost the area on chromosome 17. Additionally, the stable tumors with loss in the same region are shown. *Right,* some of the most interesting genes are shown together with their locusID. *Left,* the approximate positions of the measured SNPs are marked.

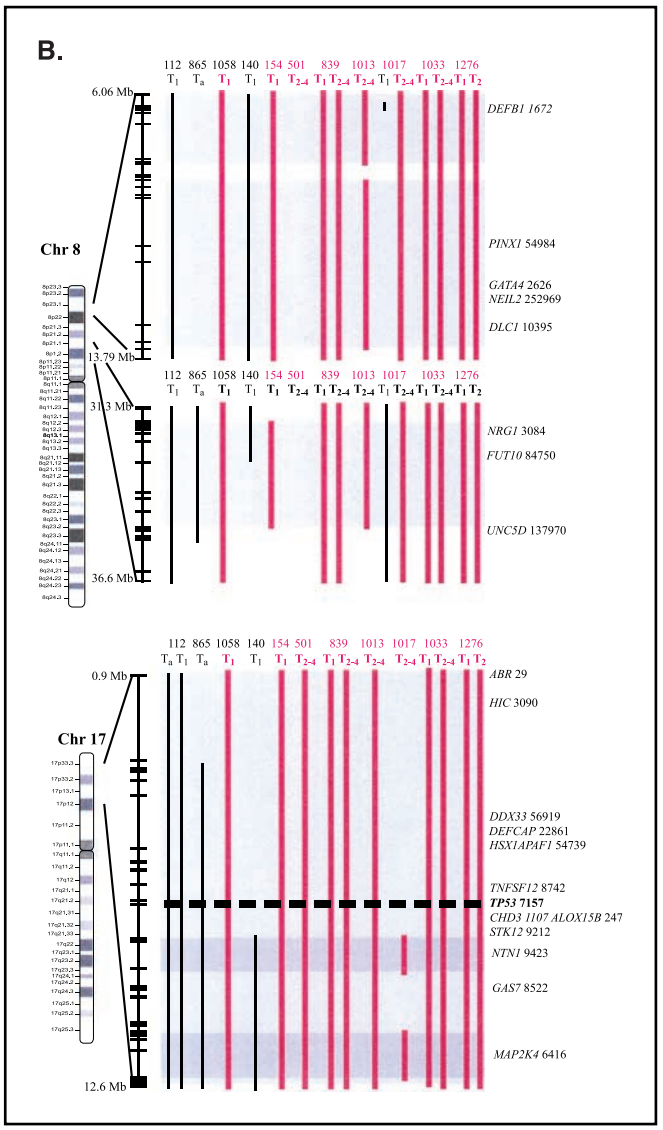

Figure 2. (continued)

detected with the presented method are almost exclusively loss of one allele. Therefore, we mainly focus on pathways and genes where loss of an allele may have a functional effect as in tumor suppressing pathways. Loss of one allele can have fatal consequences on the overall gene expression because of mutation/methylation of the other allele or haploinsufficiency (17–20). Several investigations have implicated that at least two major pathways of chromosomal loss are involved in bladder tumor development. One with loss of chromosome 9 involving the inactivation of the tumor suppressor p16 (also known as INK4A or CDKN2A). The other with loss of part of chromosome 17 and part of chromosome 13 leading to inactivation of the tumor suppressors p53 and Rb [reviewed in ref. (21)]. Alternatively, some of the areas may have AI simply due to the fact that they represent fragile chromosomal areas.

Several mechanisms have been suggested that lead to chromosomal instability such as mutations in proteins related to the anaphase-promoting complex, the telomere apparatus, etc. (22–24). However, not much is known on the causative factors.

In the present paper, we had two sets of T1 tumors, seven that had a previous superficial disease and where the T1 was the highest stage, and nine T1 tumors that were later followed by stage T2 or higher stage of invasive disease (patient 1058 developed a T2-4 tumor at a later date, which unfortunately was not available for research). Our results showed that the number of AIs were stage-dependent, which is in concert with other publications where a stage- and/or grade-dependent LOH was detected for 17p and 13q (25), for 8p and 13q (26), and for 14q and 18q (27, 28). An area at the terminal end of chromosome 15q showed only AI in T1 tumors preceded by superficial disease (4/7) and an area on chromosome 13 (44-55 Mb) showed only AI in those that were followed by muscle-invasive disease (4/10; see Fig. 2 in supplementary material). Many genes were located in the reported regions, however, no well-known tumor suppressors or oncogenes were found. These areas should be examined for their ability to predict the disease course in a larger study of bladder tumors with 5 years of follow up, and we are currently conducting such a study. As a novel finding, we also found that a large fraction of the muscle-invasive tumors had frequent AIs on chromosomes 6q, 10p, 16q, 20p, 20q, and 22q (Table 3). However, these regions do not necessarily overlap.

Our data clearly separated the tumors into two classes, those with a high genomic instability and those with a low genomic instability. Stage Ta tumors, which are superficial papillomas, all showed a low instability, having mainly chromosome 9 alterations. The superficially invasive stage T1 showed an increased number of unstable tumors and in the muscle-invasive tumors six out of nine were unstable. With the new 10,000 SNP array, we were able to characterize small regions of overlapping AI. We found that all unstable tumors had overlapping AI in an area close to the *TP53* locus at 17p and 10 out of 11 had overlapping AI in two areas at chromosome 8p. Other frequently involved overlapping chromosomal regions (AI > 50% in unstable tumors) were at chromosomes 2q, 5q, 6, 8, 9q, 10q, 11p, 13q, 17p, and 18 (Table 4).

TP53 is one of the best-characterized tumor suppressors (29). It is a key player in several of the pathways involved in cell cycle regulation and apoptosis. All but one of the unstable tumors had lost one allele at the *TP53* locus. We sequenced *TP53* in all cases and found homozygous mutations in six cases in accordance with the hypothesis that one allele was lost and the other mutated (see Table 1). This is in correspondence with our previous publication (1). We hypothesize that the inactivation of p53 is a causal factor leading to chromosomal instability. However, there is still a fraction of tumors where we, apart from the AI at 17p, do not have an explanation for the instability.

The common losses of 17p and 8p led us to scrutinize the genes in those areas. It was interesting that *Netrin-1* (*NTN1*) on chromosome 17 showed AI in all unstable tumors and that *UNC5D* on chromosome 8 showed AI in all except one, 501-5 (Fig. 2*B* and Table 1). These two molecules form ligand and receptor as netrin-1 can bind to the transmembrane receptor UNC5 family as well as to DCC (deleted in colon cancer). *UNC5D* belongs to a family of four different *UNC5* genes (*UNC5A/UNC5H1*, *UNC5B/UNC5H2/p53RDL1*, *UNC5C/UNC5H3*) that are not yet completely characterized. The UNC5 family and DCC are called dependence receptors as they share the property of inducing apoptosis in the absence of ligand, hence creating a cellular state of dependence on the ligand (30, 31). In colorectal cancer, the expression of the UNC5 proteins has been correlated with tumor suppressor activity involving three major mechanisms: LOH, promoter silencing, and absence of

p53-dependent transactivation (31). Affymetrix expression array data show decreased expression of two of the *UNC5* genes at the RNA level according to bladder tumor stage and Ta grade; however, the expression array does not contain a specific probeset for UNC5D.

The reduced expression of the *UNC5* genes may offer tumor cells a selective advantage because the lack of netrin-1 in the intercellular space would kill the cells. Reducing both netrin-1 and UNC5 simultaneously may therefore be a mechanism of survival in tumor cells. It has been proposed that netrin-1 binding activates a specific mitogen-activated protein kinase pathway (32), and as *MAP2K4* is also subjected to AI in all the unstable tumors (Fig. 2*B*) it is possible that the dependence receptor system in general is down-regulated or subjected to inactivation in bladder tumors. MAP2K4 has also been implicated as a tumor suppressor in breast cancer (33).

Instability does not seem to be a prerequisite for invasive growth as a few muscle-invasive tumors were chromosomally stable. However, it would be interesting to further characterize the pathway followed by these two tumor groups. In colorectal cancer, two groups of tumors have been defined; those that are chromosomally instable and those that are chromosomally stable but have microsatellite instability. The latter are generally located in the proximal colon, the former in the distal colon. Interestingly, we found a similarity regarding AI in our material. Only in one out of eight cases with unstable tumors UTT occurred, whereas patients with exclusively stable tumors had UTT in seven out of nine cases ($P < 0.05$). We therefore investigated whether the stable tumors had high microsatellite instability according to the five loci chosen by Suraweera and coworkers (11) as well suited to investigate microsatellite instability in colon cancer. None of the stable tumors had high microsatellite instability. In fact, none of the tested microsatellite loci showed instability (data not shown). This is in accordance with other investigations that have established that high microsatellite instability, although more common in upper lesions of UTT, is very rare in bladder cancer (14–16). Therefore, we have no apparent explanation for this puzzling coincidence of chromosomal stability in the bladder tumor and UTT.

We obtained two or three tumors from all patients and it was statistically significant that Ta and T1 tumors had less AIs in common compared with T1 and T2. When AI in Ta was compared with AI in T1, only approximately two out of three AI were reproduced in the latter tumor. This indicates a clonal evolution or a mixture of different clonal subpopulations within a given Ta tumor. A similar finding was observed by others in colorectal adenomas that showed several different microsatellite lengths, although when these progressed into a tumor, this number was reduced as if a single clone had expanded and the remaining subpopulations diminished or disappeared (34). We suggest that the transition from several tumor cell subpopulations to a single major clone occurs at the T1 stage, as T1 and T2 tumors from the same patient were much more similar than Ta and T1 tumors with respect to AIs. Two recent reviews discuss the clinical consequences of clonality in cancer research (35, 36).

In conclusion, we show an effective high-resolution scoring of AI using a 10,000 SNP array. We identified several novel chromosomal areas showing imbalance in bladder cancer in a stage-dependent fashion. Two distinct groups of tumors exist, one that is highly unstable, having a 17p imbalance, half of them characterized by homozygous *TP53* mutations.

Furthermore, we confirm previously characterized regions thus demonstrating that the method is reliable and the material is representative for bladder cancer. We show a stage-dependent pattern where a shift towards monoclonality occurs when T1 progresses to T2. Several interesting genes, such as *UNC5H* and *Netrin-1* were located in the overlapping unstable regions; however, we will have to await further functional characterization before their importance for bladder cancer progression can be established. The strong stage-related imbalance of some of the areas indicates that they might be useful as predictive markers for tumor progression.

Acknowledgments

Received 5/4/2004; revised 9/6/2004; accepted 11/2/2004.

Grant support: Supported by The Danish Cancer Society, the John and Birthe Meyer Foundation, The University and County of Aarhus, and the Danish Research Council.

The costs of publication of this article were defrayed in part by the payment of page charges. This article must therefore be hereby marked advertisement in accordance with 18 U.S.C. Section 1734 solely to indicate this fact.

We thank Mie Madsen, Inge-Lis Thorsen, Anette B. Nielsen, and Lotte Gernyx for skillful technical assistance, and Bente Pytlich and Birgitte Stougård for tissue sampling.

References

1. Primdahl H, Wikman FP, von der Maase H, Zhou XG, Wolf H, Ørntoft TF. Allelic imbalances in human bladder cancer: genome-wide detection with high-density single-nucleotide polymorphism arrays. J Natl Cancer Inst 2002;94:216–23.
2. Richter J, Jiang F, Gorog JP, et al. Marked genetic differences between stage pTa and stage pT1 papillary bladder cancer detected by comparative genomic hybridization. Cancer Res 1997;57:2860–4.
3. Veltman JA, Fridlyand J, Pejavar S, et al. Array-based comparative genomic hybridization for genome-wide screening of DNA copy number in bladder tumors. Cancer Res 2003;63:2872–80.
4. Hoque MO, Lee CC, Cairns P, Schoenberg M, Sidransky D. Genome-wide genetic characterization of bladder cancer: a comparison of high-density single-nucleotide polymorphism arrays and pCR-based microsatellite analysis. Cancer Res 2003;63:2216–22.

5. Ørntoft TF, Thykjaer T, Waldman FM, Wolf H, Celis JE. Genome-wide study of gene copy numbers, transcripts, and protein levels in pairs of non-invasive and invasive human transitional cell carcinomas. Mol Cell Proteomics 2002;1:37–45.

6. Bringuier PP, Tamimi Y, Schuuring E, Schalken J. Expression of cyclin D1 and EMS1 in bladder tumours; relationship with chromosome 11q13 amplification. Oncogene 1996;12:1747–53.

7. Richter J, Beffa L, Wagner U, et al. Patterns of chromosomal imbalances in advanced urinary bladder cancer detected by comparative genomic hybridization. Am J Pathol 1998;153:1615–21.

8. Bruch J, Wohr G, Hautmann R, et al. Chromosomal changes during progression of transitional cell carcinoma of the bladder and delineation of the amplified interval on chromosome arm 8q. Genes Chromosomes Cancer 1998;23:167–74.

9. Lindblad-Toh K, Tanenbaum DM, Daly MJ, et al. Loss-of-heterozygosity analysis of small-cell lung carcinomas using single-nucleotide polymorphism arrays. Nat Biotechnol 2000;18:1001–5.

10. Janne PA, Li C, Zhao X, et al. High-resolution single-nucleotide polymorphism array and clustering analysis of loss of heterozygosity in human lung cancer cell lines. Oncogene 2004;23:2716–26.

11. Suraweera N, Duval A, Reperant M, et al. Evaluation of tumor microsatellite instability using five quasimonomorphic mononucleotide repeats and pentaplex PCR. Gastroenterology 2002;123:1804–11.

12. Eddy SR. Profile hidden Markov models. Bioinformatics 1998;14:755–63.

13. Durbin R, Eddy SR, Krogh A, Mitchison G. Biological sequence analysis: Probabilistic models of proteins and nucleic acids. Cambridge, UK: Cambridge University Press; 1998.

14. Bonnal C, Ravery V, Toublanc M, et al. Absence of microsatellite instability in transitional cell carcinoma of the bladder. Urology 2000;55:287–91.

15. Catto JW, Azzouzi AR, Amira N, et al. Distinct patterns of microsatellite instability are seen in tumours of the urinary tract. Oncogene 2003;22:8699–706.

16. Catto JW, Meuth M, Hamdy FC. Genetic instability and transitional cell carcinoma of the bladder. BJU Int 2004;93:19–24.

17. Fodde R, Smits R. Cancer biology. A matter of dosage. Science 2002;298:761–3.

18. Santarosa M, Ashworth A. Haploinsufficiency for tumour suppressor genes: When you don't need to go all the way. Biochim Biophys Acta - Reviews on Cancer. In Press.

19. Knight JC. Allele-specific gene expression uncovered. Trends Genet 2004;20:113–6.

20. Delaval K, Feil R. Epigenetic regulation of mammalian genomic imprinting. Curr Opin Genet Dev 2004; 14:188–95.

21. Sanchez-Carbayo M. Use of high-throughput DNA microarrays to identify biomarkers for bladder cancer. Clin Chem 2003;49:23–31.

22. Doherty SC, McKeown SR, McKelvey-Martin V, et al. Cell cycle checkpoint function in bladder cancer. J Natl Cancer Inst 2003;95:1859–68.

23. Motoyama N, Naka K. DNA damage tumor suppressor genes and genomic instability. Curr Opin Genet Dev 2004;14:11–6.

24. Rajagopalan H, Jallepalli PV, Rago C, et al. Inactivation of hCDC4 can cause chromosomal instability. Nature 2004;428:77–81.

25. Habuchi T, Ogawa O, Kakehi Y, et al. Accumulated allelic losses in the development of invasive urothelial cancer. Int J Cancer 1993;53:579–84.

26. Knowles MA, Elder PA, Williamson M, Cairns JP, Shaw ME, Law MG. Allelotype of human bladder cancer. Cancer Res 1994;54:531–8.

27. Chang WY, Cairns P, Schoenberg MP, Polascik TJ, Sidransky D. Novel suppressor loci on chromosome 14q in primary bladder cancer. Cancer Res 1995;55: 3246–9.

28. Brewster SF, Gingell JC, Browne S, Brown KW. Loss of heterozygosity on chromosome 18q is associated with